Available online at www.sciencedirect.com
ScienceDirect
Journal of Environmental Sciences 2012, 24(2) 254–260
JOURNAL OF ENVIRONMENTAL SCIENCES
ISSN 1001-0742
CN 11-2629/X
www.jesc.ac.cn

Photolysis of chlortetracycline in aqueous solution: Kinetics, toxicity and products

Yong Chen[1,2], Hua Li[2], Zongping Wang[2,*], Tao Tao[2], Dongbin Wei[1], Chun Hu[1,*]

1. State Key Laboratory of Environmental Aquatic Chemistry, Research Center for Eco-Environmental Sciences, Chinese Academy of Sciences, Beijing 100085, China
2. School of Environmental Science and Engineering, Huazhong University of Science and Technology, Wuhan 430074, China.
E-mail: ychen@mail.hust.edu.cn

Received 13 April 2011; revised 10 May 2011; accepted 11 May 2011

Abstract

The aqueous photodegradation of the widely used antibiotic chlortetracycline (CTC) was investigated under simulated sunlight. The quantum yield of photodegradation increased from 3.3×10^{-4} to 8.5×10^{-3} within the pH range of 6.0 to 9.0. The presence of Ca^{2+}, Fe^{3+}, and NO_3^- enhanced the photodegradation of CTC, whereas Mg^{2+}, Mn^{2+}, and Zn^{2+} inhibited the degradation with the order Mn^{2+} > Zn^{2+} > Mg^{2+} at pH 7.3. The monovalent cations (Na^+ and K^+) had negligible effect on the photolysis of CTC. Fulvic acid (FA) decreased the photodegradation of CTC due to light screening effect. Hydrogen peroxide (H_2O_2) was formed concurrently with direct photodegradation of CTC. The generation rate of H_2O_2 increased from 0.027 to 0.086 μmol/(L·min) when the pH ranged from 6.0 to 9.0. The CTC solution was about three-fold more toxic to the *Photobacterium phosphoreum* bacteria after irradiation, suggesting that the photoproducts and H_2O_2 formed in the CTC solution exhibited high risk on the bacteria. By LC-ESI(+)-MS, the photoproducts of CTC were identified. The direct photodegradation of CTC was involved in hydroxylation and N-demethyl/dedismethyl processes. The main photoproducts included the iso-CTC analog containing hydroxyl groups (m/z 511.4 and 495.4), and the N-demethyl/dedismethyl products of the photoproduct m/z 495.4 (m/z 481.3 and 467.4). In addition, the photochemical dechlorination of CTC led to tetracycline (m/z 445.5).

Key words: chlortetracycline; direct photodegradation; phototoxicity; photoproducts
DOI: 10.1016/S1001-0742(11)60775-4

Introduction

The issue of pharmaceuticals and personal care products (PPCPs) in the aquatic environment has been a subject of increasing concern and scientific interest over the last decade. Antibiotics are one of the most important concerns of the pharmaceuticals due to their extensive use and the selection for antibiotic-resistant genes (Witte, 1998; Pruden et al., 2006). Tetracyclines ranked second in production and usage worldwide (Levy, 2002). They are commonly used as therapeutics and growth promoters in husbandry, cattle, swine, poultry and fishery, with a widespread presence in surface waters (Sanderson et al., 2005; Fritz and Zuo, 2007). The tetracycline resistance genes have been detected in aquatic system (Zhang et al., 2009; Wu et al., 2010). The potential detrimental impact of tetracyclines on aquatic ecosystem therefore made it essential to study their fate before an ecological risk assessment.

Direct photodegradation is an important elimination process for tetracyclines due to their extensive overlap with solar spectrum. Until recently, the highest concern on the direct photodegradation of tetracyclines were tetracycline and oxytetracycline. The photochemical behavior of CTC has received only limited attention in aqueous environment. Several studies documented the photodegradation of CTC in soil/water environment (Halling-Sørensen et al., 2005; Werner et al., 2009). In addition, one hydroxylation photoproduct was identified by Eichhorn and Aga (2004). Nevertheless, the other photoproducts and photodegradation process of CTC were still largely unknown.

It has been established that Fe^{3+} and NO_3^- are the common photoreactive ions for the potential to generate $^{\bullet}OH$ under sunlight (Zuo et al., 1998; Pozdnyakov et al., 2000). Accordingly, the presence of Fe^{3+} and NO_3^- may enhance the photodegradation of CTC. The other metal cations including Mg^{2+}, Ca^{2+}, Mn^{2+}, and Zn^{2+} can form metal-ions complexes with CTC (Lambs et al., 1988), thereby affecting the photodegradation of CTC. In addition, humic substances (HS) are ubiquitous in natural waters and exhibited significant effect on phototransformation of numerous pollutants (Canonica, 2007). HS acted as photosensitizes for indirect photodegradation due to the formation of reactive species, including $^1O_2$, $O_2^{\bullet-}/HO_2^{\bullet}$,

* Corresponding author. E-mail: zongpingw@yahoo.com (Zongping Wang); huchun@rcees.ac.cn (Chun Hu)

H_2O_2, e^-_{aq} and the reactive HS triplet states ($^3HS^*$) (Boule et al., 1999). However, the role of HS was complicated in direct photodegradation of organic pollutants by the contrary effects, i.e., light screening and photosensitization (Chen et al., 2008). It was not clear the combined effect of these photoreactive substances on the photodegradation of CTC.

The objectives of this study were to determine the quantum yields of direct photodegradation of CTC at various pH values and examine the effect of the environmental media including metal ions, NO_3^-, and HS on the photodegradation. The photoinduced H_2O_2 was detected and the phototoxicity of CTC was assessed via the *P. phosphoreum* bacteria. The photoproducts of CTC were identified by liquid chromatography/electrospray-mass spectrometry (LC-ESI-MS). A photodegradation pathway was proposed according to the photoproducts.

1 Materials and methods

1.1 Materials

Chlortetracycline hydrochloride (CTC, ≥ 97%) was purchased from the Sigma Chemical Corporation and used as received. Pyridine, p-nitroanisole (PNA), NaCl, KCl, $CaCl_2$, $MgCl_2{\cdot}6H_2O$, $MnCl_2{\cdot}6H_2O$, and $ZnCl_2{\cdot}6H_2O$ were supplied by Wuhan Chemicals Corporation, China. Stock solution of CTC was prepared fresh daily from the solid. All chemicals were of at least analytical-reagent grade.

1.2 Photolysis experiments

All photolysis experiments were conducted in a 60 ml cylindrical Pyrex vessel (40 mm i.d., containing 50 mL of solution) under 150-W Xenon Short Arc Lamp. The irradiation below 300 nm was cut off by the Pyrex reactor. Aliquots of samples (300 μL) were withdrawn at various intervals and substrate decay was measured by high performance liquid chromatography (HPLC).

1.3 Toxicity measurement

Photobacterium bioassay method quantified the decrease in light emission from the *P. phosphoreum* bacteria as a result of exposure to pollutants. Bacterial growth was assessed by measuring optical density at around 480 nm after a 15-min exposure in dark and compared with initial optical density (OD) of each solution, expressed by 15-min OD_{480}/initial OD_{480} (relative OD) (Wang et al., 2007). The test instrument (Model toxicity analyzer DXY-2) and the bacteria *P. phosphoreum* were obtained by the Institute of Soil Science, Chinese Academy Sciences, China. The data quantifying the relationship between the logarithmic concentration of CTC and the corresponding relative OD were fit with the Boltzmann curve fit (Wammer et al., 2006).

1.4 Analytical methods

UV-Vis spectra were recorded on a Hitachi U3100 spectrophotometer. The HPLC analyses were performed using an Alliance 2695 (Waters, USA) HPLC system with 2996 diode array detector and XTerra MS column (5 μm, 250 mm × 2.1 mm). The optimized mobile phase for CTC was 15% methanol-25% acetonitrile-60% 0.01 mol/l oxalic acid solution, and the flow rate was kept at 1 mL/min. The photodiode array detector was set at 355 nm. For PNA, the mobile phase was 50% acetonitrile-50% H_2O with the flow rate 1 mL/min. The photodiode array detector was set at 300 nm. The concentration of H_2O_2 generated in the photochemical reaction of CTC under simulated sunlight irradiation was determined with a photometric method described in the literature (Bader et al., 1988).

1.5 Photoproducts determination

The photolysis products of CTC were determined immediately after irradiation on an Alliance 2690 HPLC system equipped with a single-quadruple mass spectrometer ZQ 4000 (Micromass, Manchester, UK). The analytical column was Agilent Zorbax SB-C18 (3.5 μm, 100 mm × 2.1 mm). The separation was performed by gradient elution with mobile phase A (H_2O) containing 0.2% (V/V) formic acid and B (MeOH). The gradient was as follows: 0–6 min, a linear gradient from 90% A to 80% A, 6–12 min, 50% A, 12–18 min, 80% A, 18–20 min, 90% A, 20–30 min, 90% A. Full-scans of product ions were obtained in positive ionization mode. The mass spectrums were obtained by scanning the quadrupole from 200 to 500 m/z with a 0.6-second scan. The variable settings were: source temperature 120°C; desolvation temperature: 300°C; capillary voltage 2.5 kV; cone voltage 26 V.

2 Results and discussion

2.1 Effect of pH on photodegradation of CTC

The environmentally relevant quantum yields for photodegradation of CTC were determined using the Xenon lamp within the pH range of 6.0–9.0. The values were calculated from Eq. (1) (Dulin and Mill, 1982)

$$\varphi_s = \frac{k_s}{k_a}\frac{\sum L_\lambda \varepsilon^a_\lambda}{\sum L_\lambda \varepsilon^s_\lambda}\varphi_a \quad (1)$$

where, s is the substrate (CTC, 20 μmol/L), a is the actinometer (PNA, 20 μmol/L), k is the rate constant for direct photolysis, L_λ values (lamp irradiance at a specific wavelength) were taken from the manufacturer, ε_λ values are the molar absorptivities of the substrate (obtained from absorbance spectra) or actinometer (tabulated values from Leifer, 1988) and φ is the quantum yield of direct photolysis.

Figure S1 shows the absorption spectra of different species of CTC and the relative intensity of the Xe lamp used. There was great overlap between the absorption spectra of CTC and the light source, indicating the possibility of direct photodegradation. Moreover, the light absorption of CTC exhibited red shift (centered at 355 nm) with increasing pH and overlapped more with the spectrum of light source in the long wavelength UVA region. As shown in Fig. 1, the quantum yields for photodegradation of CTC increased from 3.3×10^{-4} to 8.5×10^{-3} within the

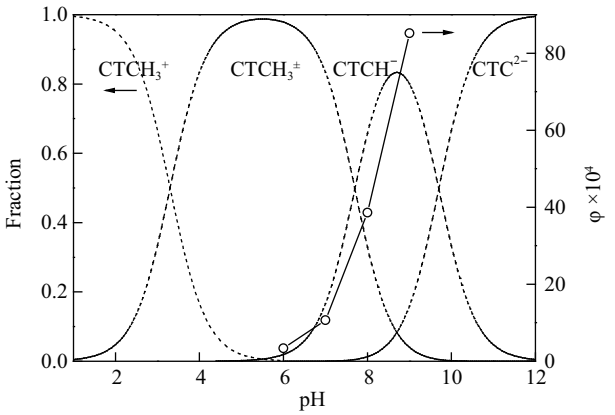

Fig. 1 Speciation-dependent quantum yields for photodegradation of CTC.

pH range of 6.0 to 9.0.

Figure S2 shows that CTC exhibited four different forms at different pH, including fully protonated form ($CTCH_3^+$), zwitterionic form ($CTCH_2^{\pm}$), monoanion ($CTCH^-$), and dianion (CTC^{2-}). The fraction of each form of CTC is illustrated in Fig. 1 according to the pK_a values of each acidic proton. Figure 1 shows that the zwitterionic state ($CTCH_2^{\pm}$) was the predominant form of CTC at pH 6.0. As the pH was raised to 9.0, CTC was gradually deprotonated from the β-hydroxyketo system at C11, C11a and C12 of the BCD ring to the dimethylamino group at C4 of CTC. The deprotonation processes of CTC led to the marked increase of photodegradation of CTC (Fig. 1). Therefore, the environmental photodegradation of CTC is susceptible to the pH of natural waters.

2.2 Ionic effect on photodegradation of CTC

As shown in Table 1, the addition of Na^+ and K^+ had negligible effect on the photolysis of CTC at pH 7.3, suggesting that the monovalent cations played insignificant role in the degradation in natural waters. It is well known that NO_3^- is a photoreactive ion to lead to $^{\bullet}OH$ under irradiation (Zuo and Deng, 1998). Table 1 shows that the addition of NO_3^- increased the photodegradation of CTC. Compared to the rapid direct photodegradation, the contribution of $^{\bullet}OH$ arising from NO_3^- to the degradation was less important. Nevertheless, the effect of NO_3^- on photodegradation of pollutants cannot be neglected, especially in nitrate-riched waters. Likewise, Fe^{3+} can photoinduce $^{\bullet}OH$ at low pH according to Eq. (2) (Pozdnyakov et al., 2000)

$$Fe(OH)^{2+} + h\nu = Fe^{2+} + {}^{\bullet}OH \quad (2)$$

However, when the pH was raised to neutral Fe^{3+} tends to precipitate and renders little photoreactivity (Wu and Deng, 2000). In this experiment, the presence of 100 μmol/L Fe^{3+} increased markedly the photodegradation of CTC at pH 7.3 (Table 1). The unexpected enhancement was possibly associated with the formation of Fe^{3+}-CTC complexes. Under irradiation, the ligand to metal charge transfer (LMCT) may occur and CTC acted as electron donor in the Fe^{3+}-CTC complexes. The LMCT processes resulted in the oxidation of CTC and thus Fe^{3+} enhanced the photodegradation. Similar results have also been documented for the photodegradation of 2,6-dimethyphenol, glyphosate, and macrolides (Mazellier et al., 1997; Chen et al., 2007; Vione et al., 2009). In addition, the $^{\bullet}OH$ formed after the LMCT processes could enhance the degradation of CTC. This result suggested that Fe^{3+} can enhance the photodegradation of CTC in Fe^{3+}-rich waters.

The other metal ions such as Ca^{2+}, Mg^{2+}, Mn^{2+}, and Zn^{2+} are also common cations in the natural waters. They can form complexes with CTC in aqueous solution (Lambs et al., 1988). Table 1 illustrates that Ca^{2+} increased the photodegradation while Mg^{2+}, Mn^{2+}, and Zn^{2+} inhibited the degradation of CTC with the order $Mn^{2+} > Zn^{2+} > Mg^{2+}$. Although it was reported that Mn^{2+} can enhance the degradation of CTC in the presence of oxygen via redox processes in dark (Chen and Huang, 2009), the contrary effect was found in the CTC solution under irradiation. This difference may be attributed to the rapid photodegradation of CTC in this study. The different inhibition effect of Mn^{2+}, Zn^{2+}, and Mg^{2+} may be related to their complexation ability with CTC. Ca^{2+} played distinct role in the photodegradation from Mg^{2+}, Mn^{2+}, and Zn^{2+}. This phenomenon was possibly attributed to the different binding sites of metal ions in the cation complexes of CTC. It has been documented that the binding sites were different for the formation of Ca^{2+} and Mg^{2+} complexes with TC at pH 7.0 (Wessels et al., 1998). A similar result was expected for CTC according to the experiments of photodegradation. In natural waters, Ca^{2+} and Mg^{2+} shows high concentration and their photochemical effect on the fate of CTC was very important.

Table 1 Effect of different ions on the photodegradation of CTC

	$k_{obs} \times 10^3$ (min^{-1})	$t_{1/2}$ (min)	Standard error ($\times 10^{-4}$)	r^2
Control	8.07	85.8	2.2	0.9967
Na^+	8.18	84.7	3.6	0.9920
K^+	8.01	86.5	3.1	0.9928
Mg^{2+}	7.52	92.2	2.2	0.9953
Ca^{2+}	10.78	64.3	4.1	0.9932
Mn^{2+}	3.09	224.3	1.7	0.9826
Zn^{2+}	5.34	129.8	2.6	0.9925
Fe^{3+}	25.51	27.2	7.0	0.9958
NO_3^-	9.53	72.7	8.2	0.9621

All the ions concentration: 100 μmol/L; CTC: 20 μmol/L; pH 7.3.

2.3 Photochemical effect of fulvic acid

Humic substances (HS) are ubiquitous in the natural waters. As shown in Fig. 2, the addition of fulvic acid (FA) decreased the photodegradation of CTC, and the inhibition increased with increasing concentration of FA at pH 7.3. In the presence of 20.0 mg/L FA, the photodegradation decreased from 8.71×10^{-3} to 5.78×10^{-3} min^{-1}, a 66.4% decrease compared to direct photodegradation in absence of FA. It is well established that HS are important photosensitizers and can generate a series of reactive species including $^{\bullet}OH$, $^1O_2$, $O_2^{-\bullet}$, H_2O_2, e_{aq}^-, and the triplet excited-state HS ($^3HS^*$) under irradiation (Boule et al., 1999). The reactive species can react with organic pollutants and lead to the abatement of contamination. The sensitization

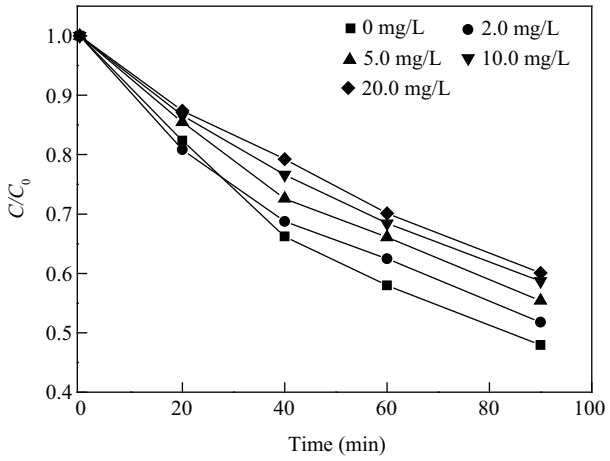

Fig. 2 Photodegradation of CTC in the presence of FA with different concentrations.

reactions are significant for indirect photodegradation. As for fast direct photodegradation, the HS also played the role of light screening to suppress the degradation. To quantify the possible effect of reactive species arising from FA on the photodegradation of CTC, a kinetic model was employed according to the following expressions (Zepp, 1978):

$$-\left(\frac{\mathrm{d}C}{\mathrm{d}t}\right)_{\lambda} = \varphi I_{0\lambda}\left(\frac{A}{V}\right)F_{s\lambda}F_{c\lambda} \tag{3}$$

where, V and A are the vessel volume and exposed area of light; $I_{0\lambda}$ is the incident light intensity at wavelength λ, $F_{s\lambda}$ and $F_{c\lambda}$ are the fraction of light absorbed by the system and CTC, respectively. The terms $F_{s\lambda}$ and $F_{c\lambda}$ are expressed by:

$$F_{s\lambda} = 1 - 10^{-(\varepsilon_{1\lambda}C_1+\varepsilon_{2\lambda}C_2)l} \tag{4}$$

$$F_{c\lambda} = \frac{\varepsilon_{1\lambda}C_1}{\varepsilon_{1\lambda}C_1 + \varepsilon_{2\lambda}C_2} \tag{5}$$

where, ε_{λ} is the extinction coefficient of 1 (CTC) and 2 (FA). The light absorption by water was negligible. According to Eqs. (3)–(5), the rate of photodegradation in the absence and presence of FA can be described as Eq. (6)) and (7), respectively:

$$-\frac{\mathrm{d}C}{\mathrm{d}t} = \int_{\lambda} \varphi I_{0\lambda}\left(\frac{A}{V}\right)(1 - 10^{-\varepsilon_{1\lambda}C_1 l}) \tag{6}$$

$$-\frac{\mathrm{d}C}{\mathrm{d}t} = \int_{\lambda} \varphi I_{0\lambda}\left(\frac{A}{V}\right)\left(1 - 10^{-(\varepsilon_{1\lambda}C_1 l+\varepsilon_{1\lambda}C_1 l)}\right)\left(\frac{\varepsilon_{1\lambda}C_1}{\varepsilon_{1\lambda}C_1 + \varepsilon_{2\lambda}C_2}\right) \tag{7}$$

The ratio of Eq. (7) and Eq. (6) was calculated to be 0.67 according to the absorption spectra of CTC (20 μmol/L) and FA (20 mg/L) (Fig. S3), and the emission spectra of the light source (Fig. S1). This suggested that the photodegradation of CTC decreased to 67% in the presence of FA (20.0 mg/L), which agreed well with the result from kinetic experiments. Therefore, the HS-photoinduced reactive species including $^{\bullet}OH$, $^1O_2$, $O_2^{\bullet-}$, H_2O_2, e_{aq}^-, and $^3HS^*$ showed little influence on the photodegradation of CTC. The decrease of photodegradation in the presence of FA was mainly attributed to the light screening effect.

2.4 Detection of H_2O_2

The photoproduction of reactive oxygen species (ROS) including $^1O_2$, $O_2^{\bullet-}$ and H_2O_2 by pharmaceuticals was crucial for the assessment of the phototoxicity in the field of therapy (Onoue et al., 2009). Likewise, it was important to assess their impact on the aquatic organisms. In this study, the formation of H_2O_2 was detected under simulated sunlight. As shown in Fig. 3, the generation rate of H_2O_2 increased from 0.027 to 0.086 (μmol/L)/min within the pH range of 6.0–9.0, corresponding to the trend of quantum yields of direct photodegradation of CTC at different pH values. This was similar to the previous research on formation of H_2O_2 from TC (Chen et al., 2008). The $^1O_2$ and $O_2^{\bullet-}$ were also detected in the irradiated CTC solution at pH 7.3 (Li et al., 1987). The ROS formed concurrently with direct photodegradation of CTC may have a potential risk on aquatic organisms, along with the photoproducts.

2.5 Phototoxicity of CTC

The toxicity of CTC solution before and after irradiation (10, 20, 30, 40, 50, 60 min) under simulated sunlight was assessed by *P. phosphoreum* bacteria after a 15-min exposure. As shown in Fig. 4, the relative OD decreased with increasing concentration of CTC and the median effective concentration (EC_{50}) of CTC was 24.1 mg/L. After irradiation, the concentration of CTC decreased, followed by the increase of photoproducts. The relative OD decreased with increasing photoproducts and the EC_{50} decreased to 7.78 mg/L, indicating the toxicity of the photoproducts was about three-fold compared to the parent compound. The inhibition experiments for *P. phosphoreum* bacteria were carried out after direct photodegradation of CTC. It is known that $^1O_2$ is a transient substance

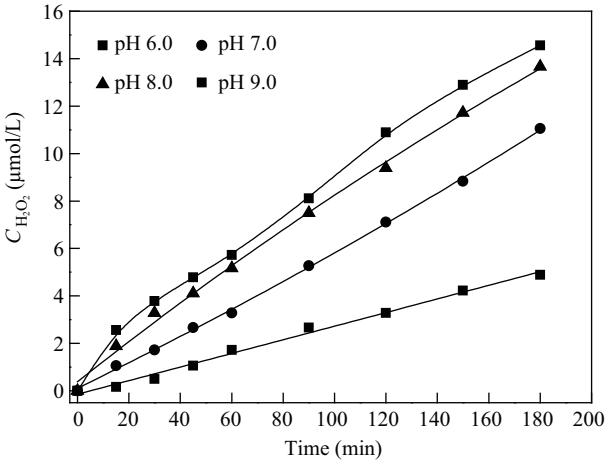

Fig. 3 Generation of H_2O_2 in the irradiated CTC solution at various pH values. Initial concentration of CTC 200 μmol/L.

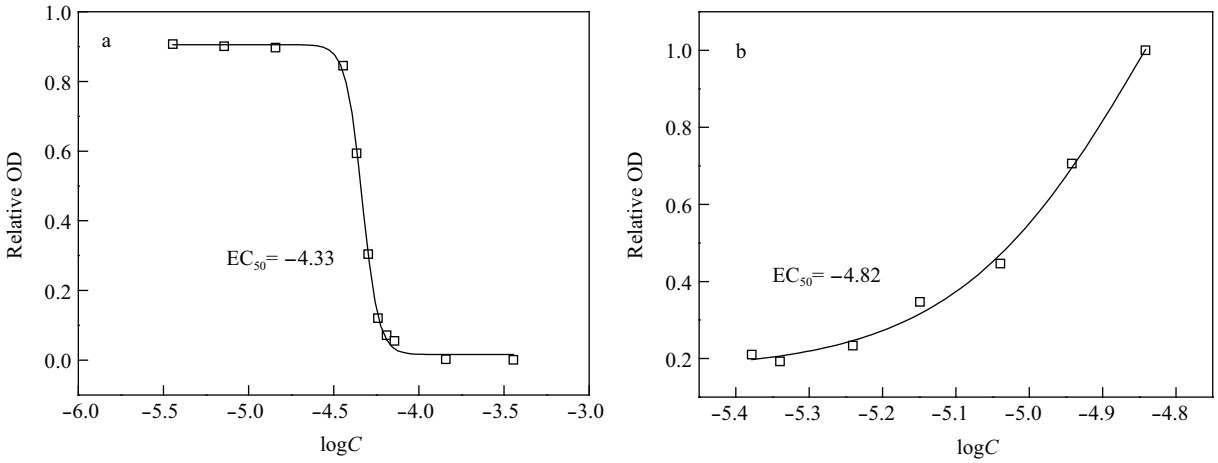

Fig. 4 Dependence of relative inhibition rate on logarithmic concentration of CTC before (a) and after irradiation (b). Solid lines corresponded to the fit according to Boltzmann function.

with lifetime about 4 μsec in aqueous solution (Rodgers and Snowden, 1982). Accordingly, the increase of toxicity after irradiation did not include the contribution of $^1O_2$ arising from self-sensitization due to its short half-life in this experiment. The production of H_2O_2 may contribute to increase of toxicity after irradiation for its continuous occurrence during the experiment. $O_2^{\bullet-}$ and H_2O_2 were reported to be generated by CTC and exhibit toxicity towards *Eschericha coli* B (Martin et al., 1987). While $O_2^{\bullet-}$ and H_2O_2 are capable of causing cell damage (Repine et al., 1981; DiGuiseppi and Fridovich, 1982), $O_2^{\bullet-}$was unlikely to be involved in toxicity in this experiment. This is because it is quite unstable in aqueous solution and undergoes very fast dismutation into H_2O_2. It is possible that the transient reactive oxygen species have *in vivo* phototoxicity towards *P. phosphoreum* bacteria in CTC solution under irradiation. Nevertheless, in this experiment the phototoxicity was largely due to the photoproducts of CTC, and possibly H_2O_2.

2.6 Determination of photoproducts

The photoproducts of CTC were detected after 60 min irradiation under simulated sunlight. Figure 5a illustrats the LC-ESI(+)-MS total ion chromatograms for the monitoring of the degradation of CTC in aqueous solution. The main photoproducts of CTC were m/z 511.4, 495.4, 481.3, 445.5, and 467.4 (Fig. S4). Apart from the product m/z 511.4, the other photoproducts were not stable and they disappeared after 24 hr in the dark (Fig. 5b). By LC/ESI-Time-of-Flight-MS, Eichhorn and Aga (2004) had identified the photoproduct m/z 511.4. The photoproduct was assigned to comprise an isoCTC-like skeleton with two additional hydroxyl groups at C11a and C5, respectively. According to the structure of the product m/z 511.4, the other photoproducts were readily identified. The m/z 495.4 was the intermediate product of m/z 511.4, which contained an isoCTC-like skeleton but with only one hydroxyl group. The most likely position for the hydroxyl group was in C11a, the first hydroxylation process for m/z 511.4 (Eichhorn and Aga, 2004).

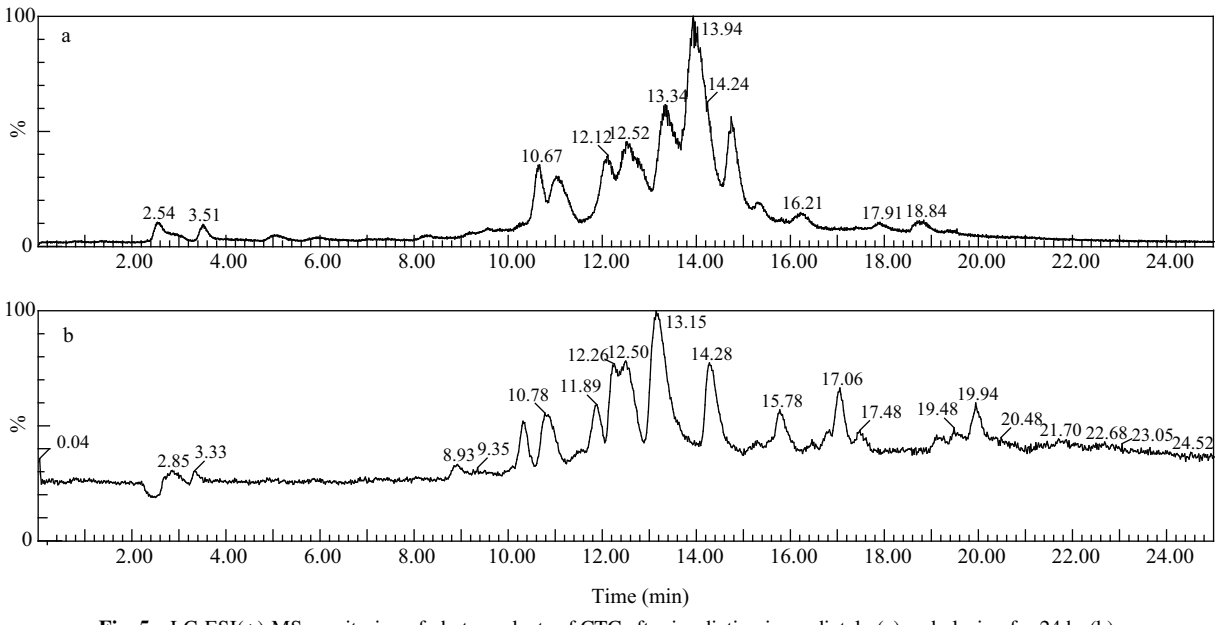

Fig. 5 LC-ESI(+)-MS monitoring of photoproducts of CTC after irradiation immediately (a) and placing for 24 hr (b).

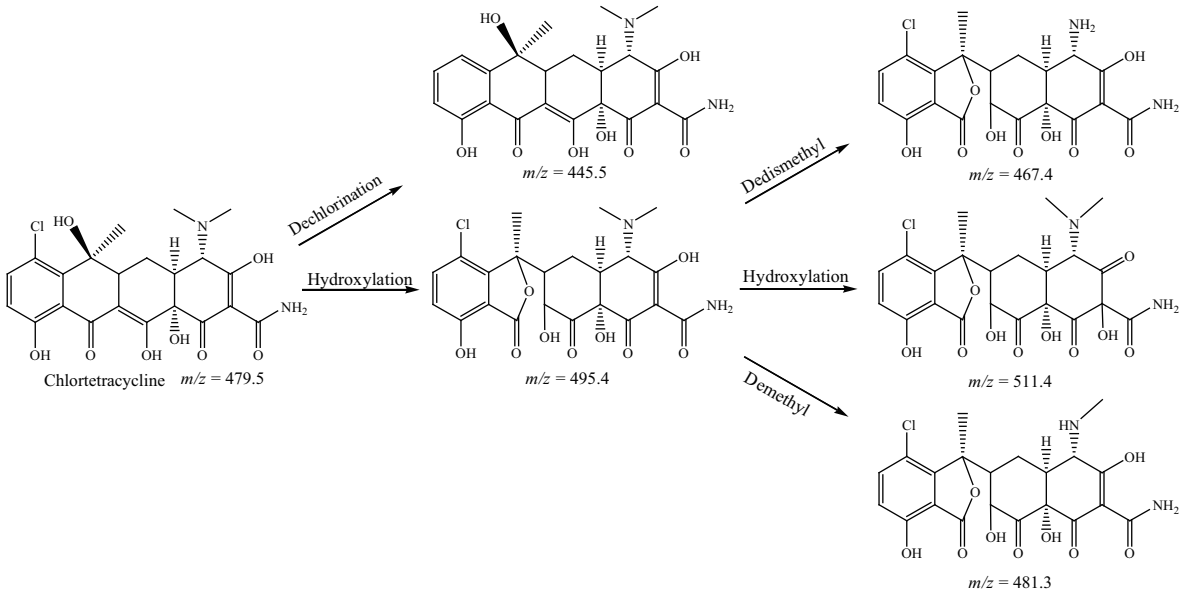

Fig. 6 Photodegradation products and pathway of CTC in aqueous solution under simulated sunlight.

The photoproducts m/z 481.3 and m/z 467.4 corresponded to the N-demethyl and dedismethyl products of m/z 495.4, respectively. In addition, tetracycline (m/z 445.5) was another important photoproduct resulting from the dechlorination of CTC. The UV-Vis and mass spectra between the authentic sample of tetracycline and the product m/z 445.5 were identical (Fig. S5), further verifying that tetracycline was the dechlorination product of CTC. Figure 6 illustrated the hydroxylation, N-demethyl/dedismethyl, and dechlorination processes of CTC during direct photodegradation under simulated sunlight.

3 Conclusions

The direct photodegradation was an important process for the abatement of CTC in surface waters. The deprotonated CTC was more susceptible to light in comparison with the protonated forms. The existence of NO_3^-, Fe^{3+}, and Ca^{2+} increased the degradation rate of CTC, while Mg^{2+}, Zn^{2+}, and Mn^{2+} decreased the photodegradation with the inhibition order $Mn^{2+} > Zn^{2+} > Mg^{2+}$. The addition of FA suppressed the degradation of CTC due to light screening effect. H_2O_2 was observed to be formed concurrently with the direct photodegradation. The irradiated solution of CTC was approximately three-fold more toxic compared to the solution before irradiation. The photodegradation of CTC was involved in the hydroxylation, N-demethyl/dedismethyl, and dechlorination processes.

Acknowledgments

This work was supported by the National Natural Science Foundation of China (No. 21007018, 51078161), the Natural Science Foundation of Hubei Province (No. 2010CDB01104), the Research Fund for the Doctoral Program of Higher Education of China (No. 20100142120004), and the 11th Five-year Plan of National Water Environmental Special Program of China (No. 2008ZX07211-10-02).

Supporting materials

Supplementary data associated with this article can be found in the online version.

References

Bader H, Sturzenegger V, Hoigné J, 1988. Photometric method for the determination of low concentrations of hydrogen peroxide by the peroxidase catalyzed oxidation of N,N-diethyl-*p*-phenylenediamine (DPD). *Water Research*, 22(9): 1109–1115.

Boule P, Bolte M, Richard C, 1999. Phototransformations induced in aquatic medium by NO_3/NO_2, Fe^{III} and humic substances. In: Handbook of Environmental Chemistry. Part 1: Environmental Photochemistry (Boule P, ed.). Springer, Berlin Heidelberg. Vol. 2: 204–205.

Canonica S, 2007. Oxidation of aquatic organic contaminants induced by excited triplet states. *Chimia International Journal for Chemistry*, 61(10): 641–644.

Chen W R, Huang C H, 2009. Transformation of tetracyclines mediated by Mn(II) and Cu(II) ions in the presence of oxygen. *Environmental Science & Technology*, 43(2): 401–407.

Chen Y, Hu C, Qu J H, Yang M, 2008. Photodegradation of tetracycline and formation of reactive oxygen species in aqueous tetracycline solution under simulated sunlight irradiation. *Journal of Photochemistry and Photobiology A: Chemistry*, 197(1): 81–87

Chen Y, Wu F, Lin Y X, Deng N S, Bazhin N, Glebov E, 2007. Photodegradation of glyphosate in the ferrioxalate system. *Journal of Hazardous Materials*, 148(1-2): 360–365.

DiGuiseppi J, Fridovich I, 1982. Oxygen toxicity in *Streptococcus sanguis*. The relative importance of superoxide and hydroxyl radicals. *Journal of Biological Chemistry*, 257(8): 4046–4051.

Dulin D, Mill T, 1982. Development and evaluation of sunlight actinometers. *Environmental Science & Technology*, 16(11): 815–820.

Eichhorn P, Aga D S, 2004. Identification of a photooxygena-

tion product of chlortetracycline in hog lagoons using LC/ESI-ion trap-MS and LC/ESI-time-of-flight-MS. *Analytical Chemistry*, 76(20): 6002–6011.

Fritz J W, Zuo Y G, 2007. Simultaneous determination of tetracycline, oxytetracycline, and 4-epitetracycline in milk by high-performance liquid chromatography. *Food Chemistry*, 105(3): 1297–1301.

Halling-Sørensen B, Jacobsen A M, Jensen J, Sengeløv G, Vaclavik E, Ingerslev F, 2005. Dissipation and effects of chlortetracycline and tylosin in two agricultural soils: a field-scale study in southern Denmark. *Environmental Toxicology and Chemistry*, 24(4): 802–810.

Lambs L, Decock-Le Reverend B, Kozlowski H, Berthon G, 1988. Metal ion-tetracycline interactions in biological fluids 9 Circular dichroism spectra of calcium and magnesium complexes with tetracycline, oxytetracycline, doxycycline, and chlortetracycline and discussion of their binding modes. *Inorganic Chemistry*, 27(17): 3001–3012.

Leifer A, 1988. The Kinetics of Environmental Aquatic Photochemistry: Theory and Practice. American Chemical Society, Washington, DC.

Levy S B, 2002. The Antibiotic Paradox (2nd ed.). Perseus Publishing, Cambridge, MA.

Li A S W, Roethling H P, Cummings K B, Chignell C F, 1987. O_2 Photogenerated from aqueous solutions of tetracycline antibiotics (pH 7.3) as evidenced by DMPO spin trapping and cytochrome c reduction. *Biochemical and Biophysical Research Communications*, 146(3): 1191–1195.

Martin J P Jr, Colina K, Logsdon N, 1987. Role of oxygen radicals in the phototoxicity of tetracyclines toward *Escherichia coli* B. *Journal of Bacteriology*, 169(6): 2516–2522.

Mazellier P, Mailhot G, Bolte M, 1997. Photochemical behaviour of the iron(III)/2,6-dimethylphenol system. *New Journal of Chemistry*, 21(3): 389–397

Onoue S, Seto Y, Oishi A, Yamada S, 2009. Novel methodology for predicting photogenotoxic risk of pharmaceutical substances based on reactive oxygen species (ROS) and DNA-binding assay. *Journal of Pharmaceutical Sciences*, 98(10): 3647–3658

Pozdnyakov I P, Glebov E M, Plyusnin V F, Grivin V P, Ivanov Y V, Vorobyev D Y et al., 2000. Mechanism of $Fe(OH)^{2+}$(aq) photolysis in aqueous solution. *Pure and Applied Chemistry*, 72(11): 2187–2197.

Pruden A, Pei R, Storteboom H, Carlson K H, 2006. Antibiotic resistance genes as emerging contaminants: studies in northern Colorado. *Environmental Science & Technology* 40(23): 7445–7450.

Repine J E, Fox R B, Berger E M, 1981. Hydrogen peroxide kills *Staphylococcus aureus* by reacting with staphylococcal iron to form hydroxyl radical. *Journal of Biological Chemistry*, 256(14): 7094–7096.

Rodgers M A J, Snowden P T, 1982. Lifetime of oxygen (O_2 ($^1\Delta_g$)) in liquid water as determined by time-resolved infrared luminescence measurements. *Journal of the American Chemical Society*, 104(20): 5541–5543.

Sanderson H, Ingerslev F, Brain R A, Halling-Sørensen B, Bestari J K, Wilson C J et al., 2005. Dissipation of oxytetracycline, chlortetracycline, tetracycline and doxycycline using HPLC-UV and LC/MS/MS under aquatic semi-field microcosm conditions. *Chemosphere*, 60(5): 619–629.

Stephens C R, Murai K, Brunings K J, Woodward R B, 1956. Acidity constants of the tetracycline antibiotics. *Journal of the American Chemical Society*, 78(16): 4155–4158.

Vione D, Feitosa-Felizzola J, Minero C, Chiron S, 2009. Phototransformation of selected human-used macrolides in surface water: Kinetics, model predictions and degradation pathways. *Water Research*, 43(7): 1959–1967.

Wammer K H, Lapara T M, McNeill K, Arnold W A, Swackhamer D L, 2006. Changes in antibacterial activity of triclosan and sulfa drugs due to photochemical transformations. *Environmental Toxicology & Chemistry*, 25(6): 1480–1486

Wang L S, Wei D B, Wei J, Hu H Y, 2007. Screening and estimating of toxicity formation with photobacterium bioassay during chlorine disinfection of wastewater. *Journal of Hazardous Materials*, 141(1): 289–294

Werner J J, McNeill K, Arnold W A, 2009. Photolysis of chlortetracycline on a clay surface. *Journal of Agricultural and Food Chemistry*, 57(15): 6932–6937

Wessels J M, Ford W E, Szymczak W, Schneider S, 1998. The complexation of tetracycline and anhydrotetracycline with Mg^{2+} and Ca^{2+}: a spectroscopic study. *Journal of Physical Chemistry B*, 102(46): 9323–9331.

Witte W, 1998. Medical consequences of antibiotic use in agriculture. *Science*, 279(5353): 996–997.

Wu F, Deng N S, 2000. Photochemistry of hydrolytic iron(III) species and photoinduced degradation of organic compounds. A minireview. *Chemosphere*, 41(8): 1137–1147

Wu N, Qiao M, Zhang B, Cheng W D, Zhu Y G, 2010. Abundance and diversity of tetracycline resistance genes in soils adjacent to representative swine feedlots in China. *Environmental Science & Technology* 44(18): 6933–6939.

Zhang W, Sturm B S M, Knapp C W, Graham D W, 2009. Accumulation of tetracycline resistance genes in aquatic biofilms due to periodic waste loadings from swine lagoons. *Environmental Science & Technology* 43(20): 7643–7650.

Zepp R G, 1978. Quantum yields for reaction of pollutants in dilute aqueous solution. *Environmental Science & Technology*, 12(3): 327–329.

Zuo Y G, Deng Y W, 1998. The near-UV absorption constants for nitrite ion in aqueous solution. *Chemosphere*, 36(1): 181–188.

Supporting materials

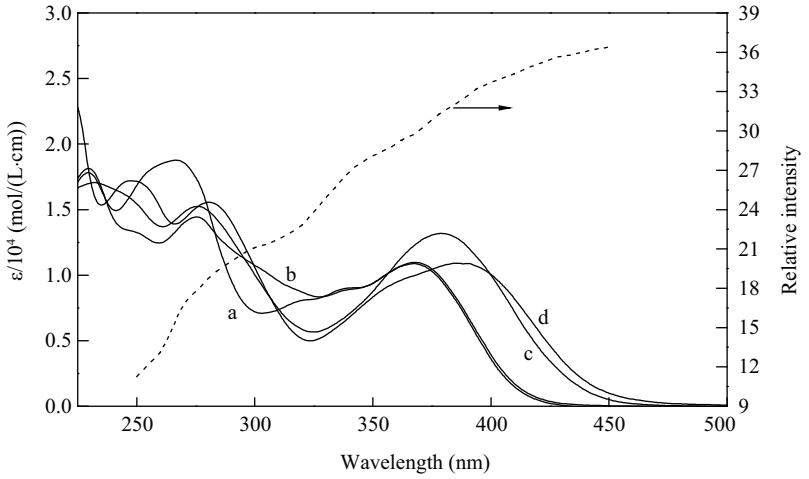

Fig. S1 Absorption spectra of different species of CTC. (line a) fully protonation form, $CTCH_3^+$; (line b) zwitterionic form, $CTCH_2^{\pm}$; (line c) monoanion, $CTCH^-$, (line d) dianion, CTC^{2-} and the relative intensity of the light source used in this work in the region that overlaps the absorption of CTC (dash line).

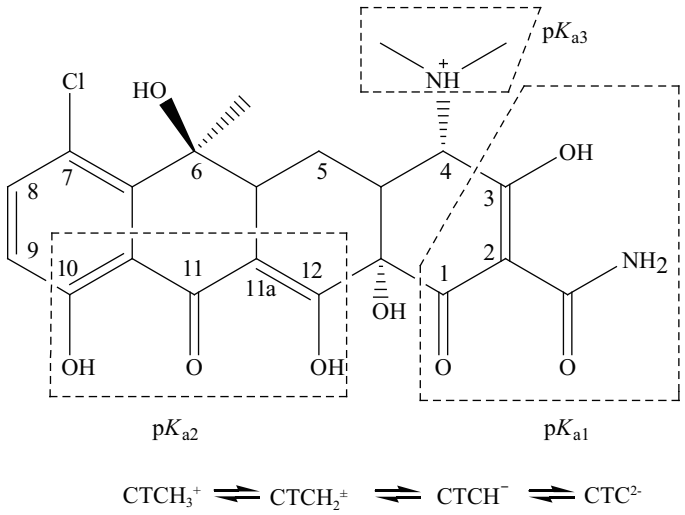

Fig. S2 Molecular structure and the different protonation/deportation equilibria of CTC. The pK_{a1}, pK_{a2} and pK_{a3} values of each acidic proton are 3.30, 7.44, and 9.27, respectively, determined by Stephens et al. (1956).

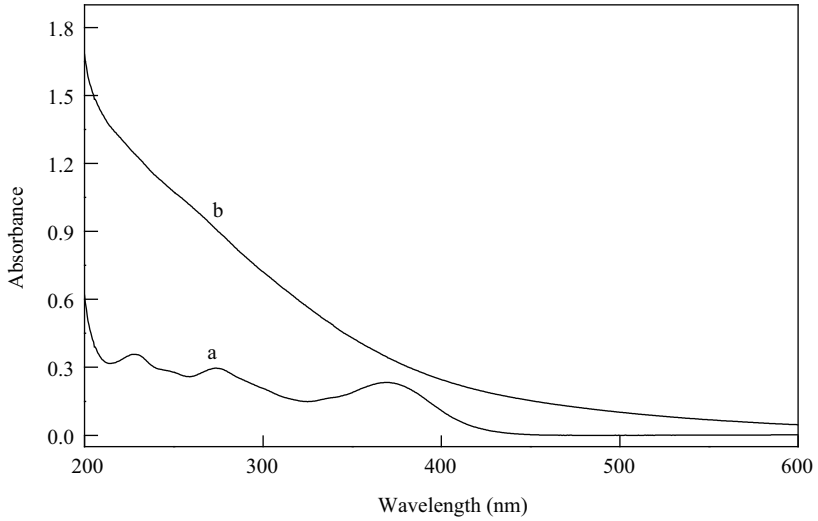

Fig. S3 The UV-Vis absorption spectra of CTC (line a,) and FA (line b). CTC 20 mol/L, FA 20 mg/L, pH 7.3.

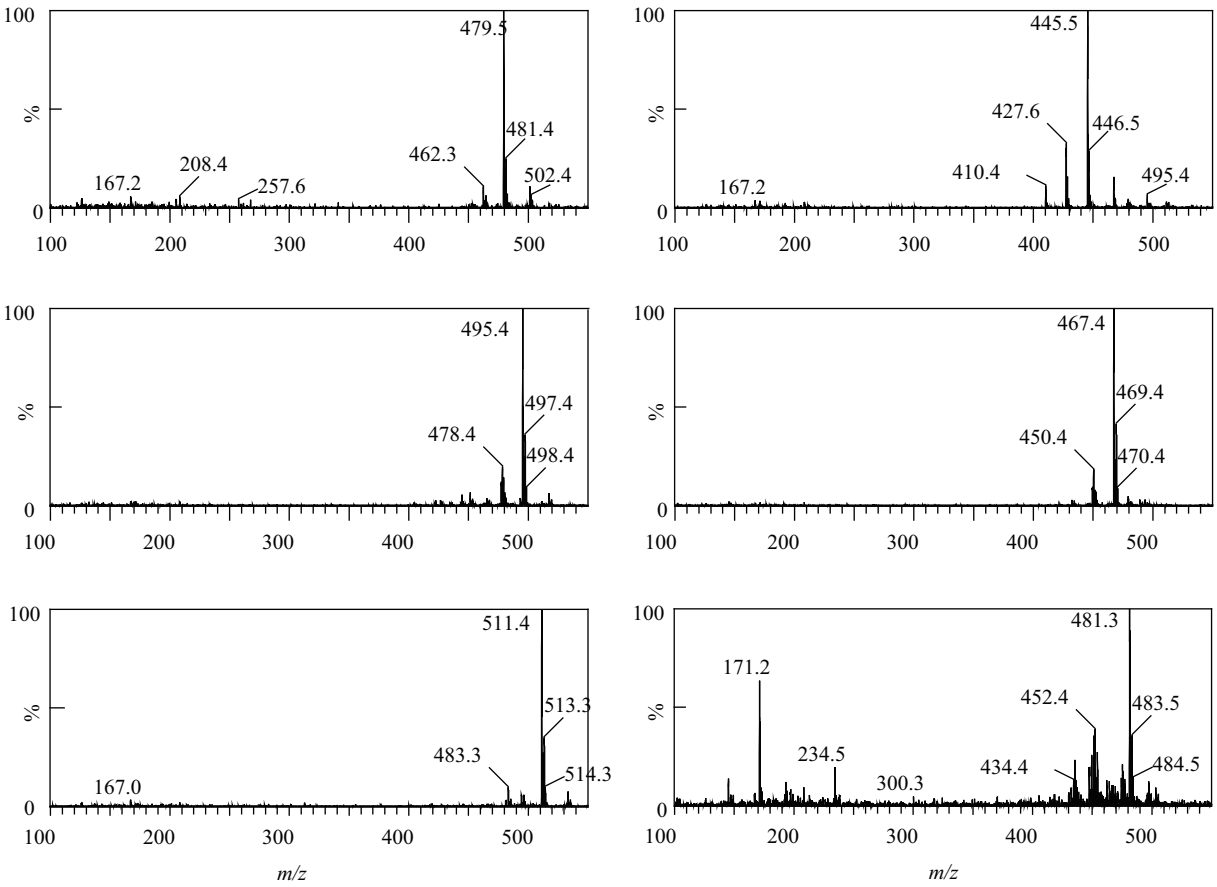

Fig. S4 ESI(+)-mass spectra of CTC and its photoproducts detected immediately after irradiation under simulated sunlight. The corresponding retention time was 10.67 min (511.4), 11.02 min (445.5), 12.24 min (495.4), 13.94 min (479.5), 14.74 min (467.4), and 16.21 min (481.3).

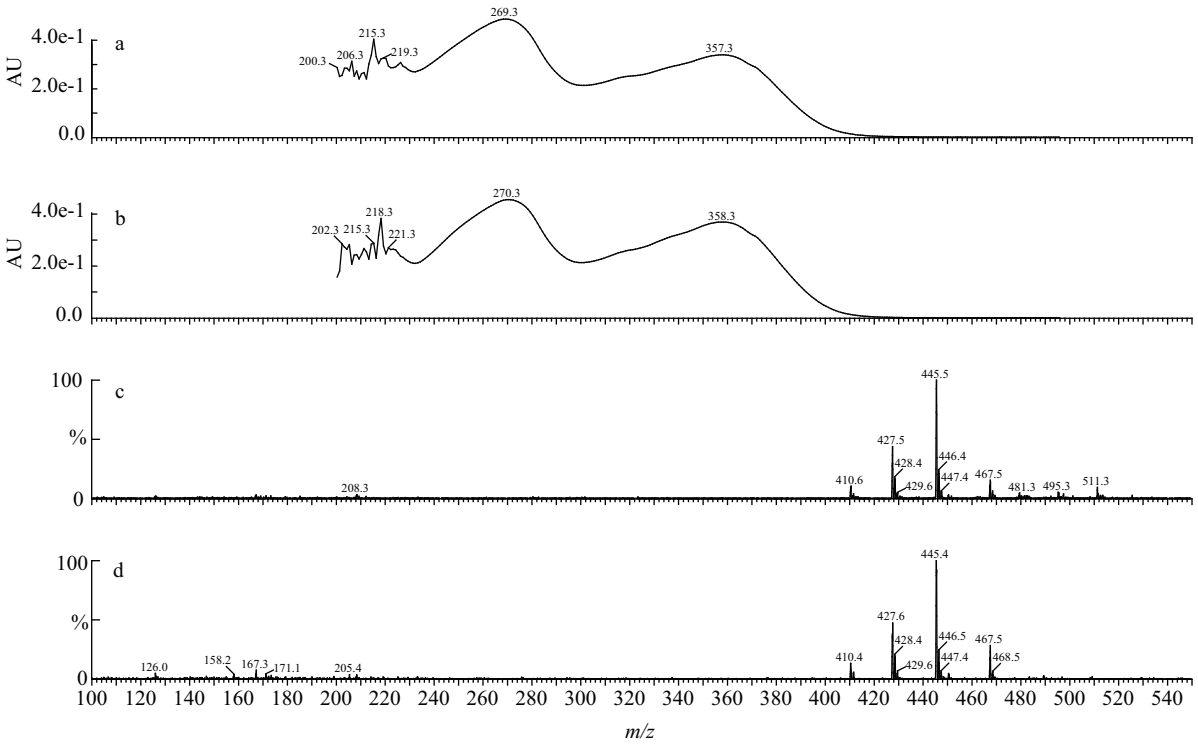

Fig. S5 Comparison of the UV-Vis and mass spectra from LC-DAD-MS data between the photoproduct (a, c) of CTC and tetracycline (b, d).